Acoustic and Electromechanical Behavior of 1-3 Piezocomposites for Ultrasonic Transducer Applications

Q. M. Zhang and Xuecang Geng
Materials Research Laboratory and Department of Electrical Engineering
The Pennsylvania State University, University Park, PA 16802

Abstract —A model is derived for the analysis of the dynamic behavior of 1-3 piezocomposites. Based on this model, the effective parameters and their dependence on the aspect ratio of the unit cell of a 1-3 composite, can be evaluated. From the model we show that the mechanical quality factor of a composite can be lower than that of both the ceramic and polymer. The predictions are compared with experimental results and the agreement between the two is quite satisfactory. verified

I. INTRODUCTION

Piezoceramic polymer composites offer many advantages over single phase materials for many transducer applications such as underwater sonar, ultrasonic imaging for medical and NDE applications, and stress sensors [1], [2]. The complementary properties of the polymer and ceramic phases in the electric and mechanical responses make it possible to tune the composite properties over a wide range.

In the past two decades, a great deal of effort have been devoted to analyze and model the transducer performance of piezocomposites. The model (quasi-static model) developed by Smith et al. [3] based on the isostrain and isostress concepts in treating the coupling between the constituent phases provided a qualitative prediction on the effective parameters of 1-3 composites. Auld et al. pointed out the existence of the stop band edge resonance in both 2-2 and 1-3 composites due to the periodic arrangement of the ceramic elements in these composites [4]. However, in order to quantitatively address many realistic issues of a composite material such as the influence of the aspect ratio of a unit cell on the performance of transducer, finite element method (FEM) is often used [5].

More recently, based on the guided wave approach, an analytical model was developed which is capable of treating many practical issues related to the ultrasonic performance of a 2-2 composite. By combining this with the eigenmode expansion, the ultrasonic properties of a finite thickness 2-2 composite can be analyzed quantitatively and many new features were predicted and confirmed experimentally [6]. It is the objective of this work to extend the model to 1-3 piezocomposites.

To simplify the mathematics of the problem, we will make use of the concentric unit cell to approximate a 1-3 composite which is shown in Fig. 1. Based on this, the ultrasonic properties related to the thickness resonance will

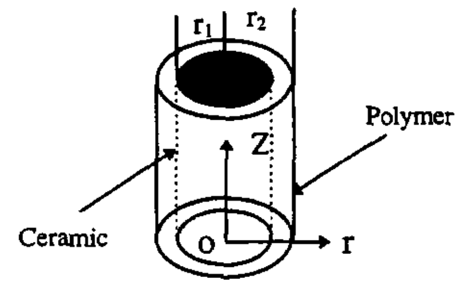

Fig. 1. Schematic drawing of one unit cell of 1-3 piezocomposite

be evaluated and compared with experiment. We will pay special attention to the mechanical Q in a composite material

II. WAVE PROPAGATION IN AN UNBOUNDED 1-3 COMPOSITE

For the unit cell shown in Fig. 1, the axial-symmetry along the poling direction of piezoceramic (the z-direction) reduces this three dimensional problem to a two dimensional one. The cylindrical coordinate system is chosen such that the z-axis is along the poling direction of the piezoceramic rod, the r-axis is along the radial direction and the θ-axis is perpendicular to the r-z plane, respectively. Because of the axial-symmetry, all the properties do not depend on the θ-coordinate and hence, the governing equations for the dynamics of a 1-3 piezo-composite become

$$\frac{\partial T_{rr}}{\partial r}+\frac{\partial T_{rz}}{\partial z}+\frac{1}{r}(T_{rr}-T_{\theta\theta})=\rho\frac{\partial^2 u_r}{\partial t^2} \quad (1a)$$

$$\frac{\partial T_{rz}}{\partial r}+\frac{T_{rz}}{r}+\frac{\partial T_{zz}}{\partial z}=\rho\frac{\partial^2 u_z}{\partial t^2} \quad (1b)$$

$$\frac{\partial D_r}{\partial r}+\frac{1}{r}D_r+\frac{\partial D_z}{\partial z}=0 \quad (1c)$$

The symbols adopted in this paper are summarized as follows: T_{ij} and S_{ij} are the stress and strain tensor components, u_i is the elastic displacement vector, ρ is the density, D_i is the electric displacement vector and E_i the electric field. The relevant material coefficients are: e_{ij} is the piezoelectric coefficient, c_{ij} is the elastic stiffness, and

0-7803-4153-8/97/$10.00

ε_1 the dielectric permittivity. Equation (1) holds for both polymer and piezoceramic phases.

The constitutive equations for the piezoceramic in the cylindrical coordinate system are

$$T_{rr} = c_{11}^E \frac{\partial u_r}{\partial r} + c_{12}^E \frac{u_r}{r} + c_{13}^E \frac{\partial u_z}{\partial z} - e_{31}E_z \tag{2a}$$

$$T_{\theta\theta} = c_{12}^E \frac{\partial u_r}{\partial r} + c_{11}^E \frac{u_r}{r} + c_{13}^E \frac{\partial u_z}{\partial z} - e_{31}E_z \tag{2b}$$

$$T_{zz} = c_{13}^E \frac{\partial u_r}{\partial r} + c_{13}^E \frac{u_r}{r} + c_{33}^E \frac{\partial u_z}{\partial z} - e_{33}E_z \tag{2c}$$

$$T_{rz} = c_{44}^E (\frac{\partial u_r}{\partial z} + \frac{\partial u_z}{\partial r}) - e_{15}E_r \tag{2d}$$

$$D_r = e_{15}(\frac{\partial u_r}{\partial z} + \frac{\partial u_z}{\partial r}) + \varepsilon_{11}^S E_r \tag{2e}$$

$$D_z = e_{31}(\frac{\partial u_r}{\partial r} + \frac{u_r}{r}) + e_{33}\frac{\partial u_z}{\partial z} + \varepsilon_{33}^S E_z \tag{2f}$$

For the polymer phase, e_{ij} in (2) is zero. The superscripts E and S indicate that the coefficients are under the constant E field and constant strain conditions, respectively. Under the quasi-electrostatic approximation, the electric field E is related to the electrical potential Φ

$$\bar{E} = -\nabla\Phi . \tag{3}$$

Combining (1), (2), and (3) yields three differential equations governing the elastic displacement u_r, u_z, and the electrical potential Φ in the piezoceramic rod and in the polymer, respectively [6]. The general solutions for the piezo-active modes in the ceramic rod have the form:

$$u_z^c = \sum_i R_i^c f_i^c J_0(h_i^c r) sin(\beta z)$$
$$u_r^c = \sum_i R_i^c g_i^c J_1(h_i^c r) cos(\beta z) \tag{4}$$
$$\Phi^c = \sum_i R_i^c t_i^c J_0(h_i^c r) sin(\beta z)$$

where i runs from 1 to 3 and the superscript c denotes the ceramic. J_0 and J_1 are the zeroth and first order Bessel functions. For each β, there are three h, h_1^c, h_2^c and h_3^c, corresponding to the quasi-electromagnetic, quasi-longitudinal, and quasi-shear waves in the piezoceramic rod, respectively. f_i^c, g_i^c and t_i^c are the ratios of the eigen vectors [6].

Similarly, the solutions for the polymer phase can be obtained [6].

The boundary conditions at the ceramic polymer interface ($r=r_1$) are

$$u_r^c = u_r^p,\ u_z^c = u_z^p,\ T_{rr}^c = T_{rr}^p,\ T_{rz}^c = T_{rz}^p \tag{5a}$$

$$\Phi^c = \Phi^p,\ D_r^c = D_r^p \tag{5b}$$

and the symmetry conditions at $r=r_2$ require

$$T_{rz}^p = 0,\ u_r^p = 0,\ D_r^p = 0 \tag{5c}$$

From (5), the relationship between ω and β, the dispersion relations, can be determined.

III. Effective Properties of a 1-3 Piezocomposite

The longitudinal wave velocity of a 1-3 composite is determined from the dispersion curves using $V_{ph}=\omega/\beta$ [6]. Presented in Fig. 2(a) are the comparison of the theoretical and experimental results of the longitudinal wave velocity V^D vs. d/t (t is the thickness) for a 1-3 composite with 40.5% ceramic volume fraction. The experimental results are obtained by the resonance method for the 1-3 composite plate at different thickness t and $V^D=2f_p t$ (f_p is the parallel resonance frequency). The agreement is very good when d/t is less than 0.65. At d/t higher than 0.65, the experimental values deviate from that of the theoretical one. This is due to the lower lateral mode frequency from the experimental samples.

Shown in Fig. 2(b) is the dependence of the longitudinal wave velocity on ceramic volume fraction for a 1-3 composite with different βr_2, a parameter inversely proportional to the aspect ratio of the unit cell. The lowering of V^D for $\beta r_2=1.0$ which is shown at the low ceramic volume content region in the figure is due to the coupling of the thickness mode with the lateral mode. For composite with higher ceramic volume fraction, this coupling will occur at higher βr_2. Hence, away from the coupling region, V^D exhibits very little dispersion. For the comparison, V^D from quasi-static model are also shown in Fig. 2(b).

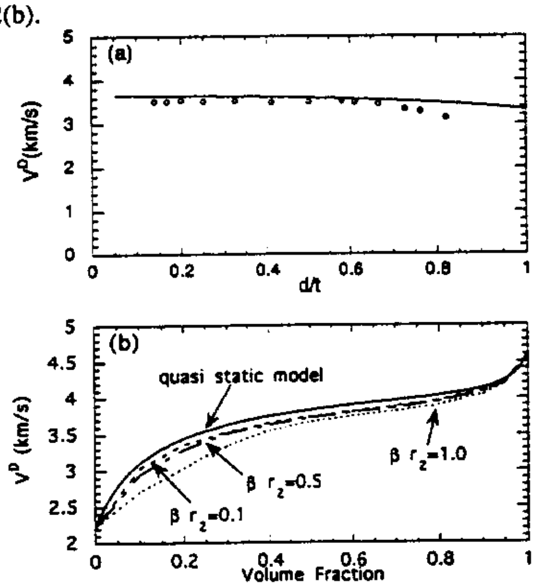

Fig. 2.(a) Longitudinal wave velocity of a 1-3 piezocomposite with 40.5% ceramic content as a function of d/t. The open circles are the experimental results and solid line is from the model. (b) The longitudinal wave velocity as a function of ceramic volume fraction for composites with different βr_2. For the comparison, the result from the quasi-static model is also included.

The thickness mode electromechanical coupling coefficient of a 1-3 piezocomposite is derived in the model from

$$k_t^2 = 1-\left(\frac{v_l^E}{v_l^D}\right)^2 \qquad (6)$$

where v_l^E *and* v_l^D are the longitudinal wave velocity under constant E and constant D conditions, respectively. Presented in Fig. 3(a) is the dependence of k_t on ceramic volume fraction for a 1-3 piezocomposite with different βr_2. Again, the reduction in k_t at the low ceramic volume fraction region for the curve with $\beta r_2 = 1$ is due to the coupling to the lateral mode. At βr_2 away from the coupling region, k_t exhibits very little dispersion. For the comparison, the results from the quasi-static model is also presented in the figure.

The thickness coupling factor for a 1-3 piezocomposite with 40.5% ceramic volume content was evaluated experimentally using the relation:

$$k_t = \frac{\pi}{2}\frac{f_s}{f_p}\tan\left(\frac{\pi}{2}\frac{f_p-f_s}{f_p}\right) \qquad (7)$$

where f_s and f_p are the series and parallel resonance frequencies of the 1-3 piezocomposite plate, respectively. The dependence of the theoretical and experimental electromechanical coupling coefficient k_t on the aspect ratio t/d is shown in Fig. 3(b) for composites with 40.5% ceramic content. The agreement between the two is excellent for d/t less han 0.65. At d/t above 0.65, the deviation of the theoretical value from the experimental one is due to the lower lateral mode frequency of the experimental samples as has been pointed out earlier.

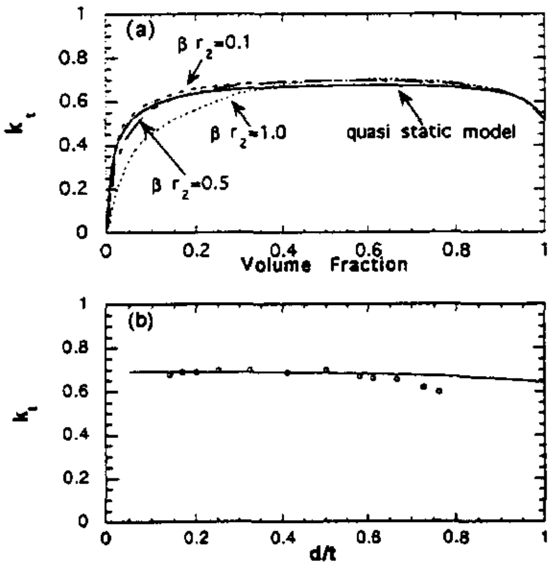

Fig. 3. (a) The electromechanical coupling coefficient k_t as a function of ceramic volume fraction for composites with different βr_2. For the comparison, the result from the quasi-static model is also included as the solid line. (b) The electromechanical coupling coefficient k_t of a 1-3 piezocomposite with 40.5% ceramic content as a function of d/t. The open circles are the experimental results and solid line is from the model.

IV. Losses in 1-3 Piezocomposites

In the previous sections, the losses in the materials have not been included. However, as has been demonstrated in many experiments, loss in a 1-3 piezocomposite is much higher than that in piezoceramic, and therefore, it is very important to include the losses in the analysis.

In general, there are three kinds of losses in a piezoelectric material, i.e. mechanical loss, dielectric loss and piezoelectric loss. In the polymer phase, there are only mechanical loss and dielectric loss. The losses in the ceramic phase can be expressed by complex constants [7],

$$c_{ij}^E = c_{ij}^{E'} + jc_{ij}^{E''},\ e_{ij} = e'_{ij} + je''_{ij} \text{ and } \varepsilon_{ij}^S = \varepsilon_{ij}^{S'} - j\varepsilon_{ij}^{S''} \qquad (8)$$

and the losses in the polymer phase can be expressed as

$$c_{ij} = c'_{ij} + jc''_{ij} \text{ and } \varepsilon = \varepsilon' - j\varepsilon'' \qquad (9)$$

From the fact that the attenuation in piezoceramic is proportional to frequency, the imaginary part of the parameters in the ceramic can be assumed constants [8]. While in the polymer phase, the main loss mechanism is due to viscosity, therefore, $c''_{ij} = \omega\eta_{ij}$, where η_{ij} is the viscosity coefficient of the polymer.

The quality factor Q (or the mechanical Q) for the thickness mode of a 1-3 piezocomposite is evaluated from the dispersion curves from the relation:

$$Q = \frac{\beta_r}{2\beta_i} \qquad (10)$$

Where β_r and β_i are the real and imaginary part of the wave vector β, respectively. Presented in Fig. 6 is the Q of a 1-3 piezocomposite as a function of the ceramic volume fraction evaluated at βr_2=0.1. The loss parameters used in the calculation are those of PZT-5H for the ceramic phase and Spurr epoxy for the polymer (listed in table I).

The results in Fig. 4 show that the quality factor of a 1-3 piezocomposite is less than that of both the ceramic and polymer for the composites evaluated. For the comparison, the quality factor for the thickness mode of several 1-3 composites with different ceramic content and single phase PZT-5H ceramic plate was experimentally determined. The experiment data is also presented in the figure which is consistent with the theoretical results. The lower value of the experimental Q for single phase PZT-5H ceramic plate compared with that from the model may be the main reason for the lower Q of the experimental samples compared with model results. The result here is quite different from the real part of the elastic constant of a 1-3 composite which always lies in between the two end phases. This is also in contrary to the common belief that the low mechanical Q in a 1-3 composite is a result of the loss in the polymer phase. In fact, in the composite evaluated, the mechanical Q of the polymer phase (Spurr epoxy) is much higher than that of the piezoceramic, while the Q of the 1-3 composite is lower than that of the pizeoceramic. The similar conclusion can also be obtained from the quasi-static model, which is presented in Fig. 5, where the quality factor is equal to 1/tanδ of $\bar{c}_{33}^{D}$ (the effective elastic constant of the composite at the constant electric displacement D).

Clearly, the coupling between the ceramic and polymer in a composite changes the phase relationship between the stress and strain in both phases. Shown in Fig. 5 is the phase angle δ between the stress (T_{zz}) and strain (S_{zz}) along the z-direction at the polymer center ($r=r_2$) and ceramic rod center (r=0) as a function of ceramic volume fraction. Apparently, for the polymer phase, the δ is reduced when the polymer is in the composite, and for the ceramic, it is increased in the composite. Hence, the large increase of the δ in the ceramic phase of the composite is the main reason for the drop in the quality factor of composites since the high elastic constants in the ceramic phase implies that the loss in the ceramic region plays a dominant role in controlling the mechanical Q of the thickness mode of a composite.

V. SUMMARY

A dynamic model is derived based on guided wave propagation method. From this model, the effective electromechanical properties of the 1-3 piezocomposites has been analyzed and show excellent agreement with experiment. It is also found the mechanical quality factor of a 1-3 composite is less than that of both ceramic and polymer phases while the mechanical quality factor of the polymer phase is larger than that of the ceramic phase. The interaction between ceramic and polymer phase changes the phase delay between stress and strain.

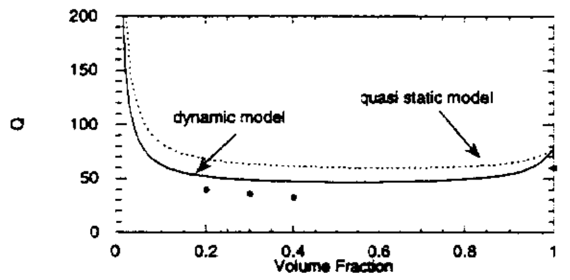

Fig. 4. Quality factor Q of 1-3 piezocomposites as a function of ceramic volume fraction. Q is evaluated at βr_1 = 0.1 and f=117 kHz (η_{11}=20.737 N/m^2 s and η_{44}=10.994 N/m^2 s for the polymer). The experimental data is represented as black dots.

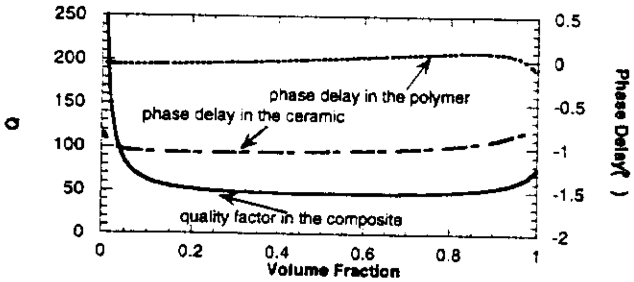

Fig. 5. The change of the phase delay δ in the center of the polymer region and the center of the ceramic region of a composite as a function of the ceramic volume content. The polymer has a Q=2222 and the calculation is carried out at βr_2=0.1. The corresponding quality factor of the composite is also included in the figure.

Table I. The material parameters for the PZT-5H and Spurr epoxy used in the model calculation

Ceramic:

$c_{11}^{E}=12.72\times10^{10}(1.0+j8.0\times10^{-3})$ N/m^2, $c_{33}^{E}=11.74\times10^{10}(1.0+j8.0\times10^{-3})$N/m^2,

$c_{12}^{E}=7.95\times10^{10}(1.0+j6.5\times10^{-3})$ N/m^2, $c_{13}^{E}=8.47\times10^{10}(1.0+j6.5\times10^{-3})$ N/m^2,

$c_{44}^{E}=2.3\times10^{10}(1.0+j1.2\times10^{-2})$ N/m^2; $\varepsilon_{11}^{S}=1700\varepsilon_0(1.0-j2.7\times10^{-2})$,

$\varepsilon_{33}^{S}=1470\varepsilon_0(1.0-j2.7\times10^{-2})$, $e_{33}=23.09(1.0-j5.4\times10^{-3})$ C/m^2,

$e_{15}=17.0(1.0-j5.0\times10^{-3})$ C/m^2, $e_{31}=-6.6(1.0-j7.2\times10^{-3})$ C/m^2, $\rho^{c}=7500$ kg/m^3.

Polymer:

$c_{11}^{p}=5.41\times10^{9}$ N/m^2, $c_{44}^{p}=1.307\times10^{9}$ N/m^2, η_{11}=20.74 N/m^{2}s,

η_{44}=11.0 N/m^{2}s; $\varepsilon_{11}^{p}=4.0\varepsilon_0$, ρ^{p}=110 0 kg/m^3.

REFERENCES

[1]. R. Newnham, "Composite Electroceramics", Ann. Rev. Mater. Sci., Vol. 16, pp. 47-68, 1986.

[2]. W. A. Smith, " The application of 1-3 piezocomposites in acoustic transducers," Proc. IEEE ISAF, Urbana, Illinois, 1990, pp. 145-152.

[3]. W. A. Smith and B. A. Auld, "Modeling 1-3 composite piezoelectrics: Thickness-mode oscillations," IEEE Trans. Ultrason., Ferroelect., Freq. Contr., Vol. 38, pp. 40-47, 1988.

[4]. B. A. Auld, H. Kunkel, Y. A. Shui, and Y. Wang, "Dynamic behavior of periodic piezoelectric composites," Proc. IEEE Ultrason., Symp., Atlanta, GA, 1983, pp. 554-558.

[5]. M. Yamaguchi, K. Y. Hashimoto, and H. Makita, "Finite element method analysis of dispersion characteristics for the 1-3 type piezoelectric composites," Proc. IEEE Ultrason., Symp., Denver, CO, 1987, pp. 657-661.

[6]. X. Geng and Q. M. Zhang, "Evaluation of Piezocomposites for Ultrasonic Transducer Applications—Influence of the Unit Cell Dimensions and the Properties of Constituents on the Performance of 2-2 composites", IEEE Trans. Ultrason., Ferroelect., Freq. Contr., Vol. 44, pp. 857-872, 1997.

[7]. R. Holland, "Representation of Dielectric, Elastic, and Piezoelectric Losses By Complex Coefficients," IEEE Trans. on Sonics and Ultrasonics, Vol. SU-14, pp. 18-20, 1967.

[8]. A. G. Evans, B. R. Tittman, L. Ahlberg, B. T. Khuri-Yakub and G. S. Kino, "Ultrasonic Attenuation in Ceramics," J. Appl. Phys. Vol. 49(5), pp. 2669-2679, 1978.